

The Taron Cesium-Thallium Epithermal Geyserite Deposit, Salta Province, Argentina

David Trueman¹, Bruce Downing², Taylor Ledoux³ and Tom Richards⁴

¹ 3560 Bunting Avenue, Richmond, BC, Canada V7E 5W1; ² 20200 Grade Crescent, Langley, BC, Canada V3A 4J6; ³ Mineral Deposits Research Unit, University of British Columbia, Vancouver, BC; ⁴ 1747 2nd Avenue NW, Calgary, AB, Canada T2N 0G2

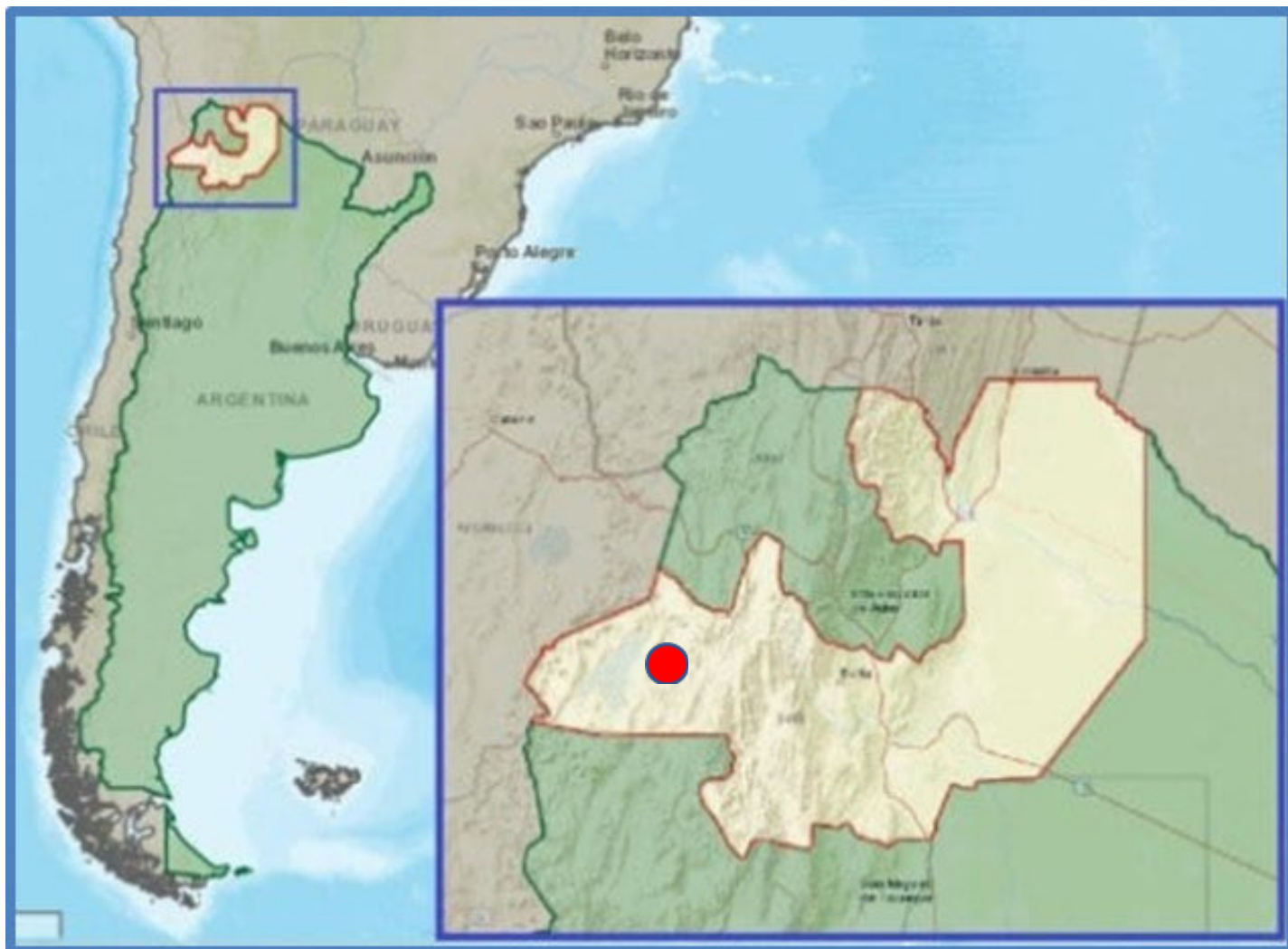
<https://doi.org/10.70499/MCQA2172>

Introduction

The Taron cesium-thallium deposit in Salta Province, Argentina (Fig.1 and inset map) (Richards 2005) is a newly recognized type of deposit that is enriched in cesium (Cs) with highly anomalous concentrations of thallium, arsenic, and manganese. The deposit was formed during a Miocene epithermal event which erupted in hot spring geyser activity forming a variety of minerals, colloids, glasses, and clays collectively termed geysersites. Albeit inactive, the Taron deposit is one of 12 other deposits in the Salta Province which display cesium enrichment. The area itself is one of 4 global locales where cesium enrichment has been documented inclusive of Tibet (Zhao *et al.* 2008), India (Chowdry *et al.* 1974) and Yellowstone National Park, Wyoming (Bargar & Beeson 1981; Dahlquist 2017).

The Taron Cs-Tl deposit was a litho-geochemical discovery, found during regional exploration by geologists working for a Vancouver-based exploration company. Prior to this work targeted for precious metals in Salta Province, geologists working for Cascadero Copper Inc. had recognized the association of silver with manganese deposits in the area and routine geochemical sampling of described manganese deposits led to the discovery of Taron in 2004. The discovery was based on ACME Analytical Laboratories and subsequently, Bureau Veritas, 60-element ICP-ES analysis which fortuitously included Cs as an additional element in the exploration package.

Figure 1. Location map of the Taron Cs deposit circled in red (inset map) in Salta Province, Argentina.



The Taron Cesium-Thallium Epithermal Geyserate Deposit... *continued from page 13*

The Taron property (Fig. 2) is about 50 km south of the village of Pocitos on the railroad between Antofagasta, Chile and the city of Salta. It is accessible by vehicle over poorly maintained roads or by helicopter.



Figure 2. Panoramic view of the Taron Cs-Tl deposit. White and off-white triangles are 10 metre backhoe trench samples (photo courtesy of T. Richards).

Geology and Mineralogy

The Taron deposit occurs within the Ochaqui Basin, an informal name assigned to the graben-like structure composed of Miocene (Simpson 2017) sedimentary and volcanic rocks. Predominant rock types include derived mudstones, arkosic, lithic and volcanic wackes with intercalated conglomeratic facies; one of which contains pebble to boulder sized clasts of orbicular granodiorite derived from the Precambrian basement rock of the Faja Irruptiva (Fig. 3). Other conglomerates contain thinly laminated pebble to cobble sized clasts derived from the Proterozoic Puncovascana Group schists.

continued on page 15

Note: This EXPLORE article has been extracted from the original EXPLORE Newsletter. Therefore, page numbers may not be continuous and any advertisement has been masked.

The Taron Cesium-Thallium Epithermal Geyselite Deposit... *continued from page 14*

All of the above rock types form an unconformable valley fill (Fig. 3) set in a graben structure bound by high angle faults that form its eastern contact. To the west, lying in unconformity, are manganese clastic rocks that hosted several, now closed, manganese mines. These rocks overlie the Faja orbicular granodiorite and in turn are cut by dykes and veins of cryptomelane and hollandite.



Figure 3. Cross section showing chaotic nature of valley fill at Taron. The black horizon is manganese stained. Stratigraphic section is approximately 3 metres in thickness. (photo courtesy of T. Richards).

Petrographic, XRD and SEM studies have been conducted at Taron by Hamilton (2005), LeCouteur (2009), and Ledoux *et al.* (2020). The deposit is dominated by cryptocrystalline silica, manganates, arsenates, and oxides (Fig. 4, Table 1). Collectively, these are known as geyselites.

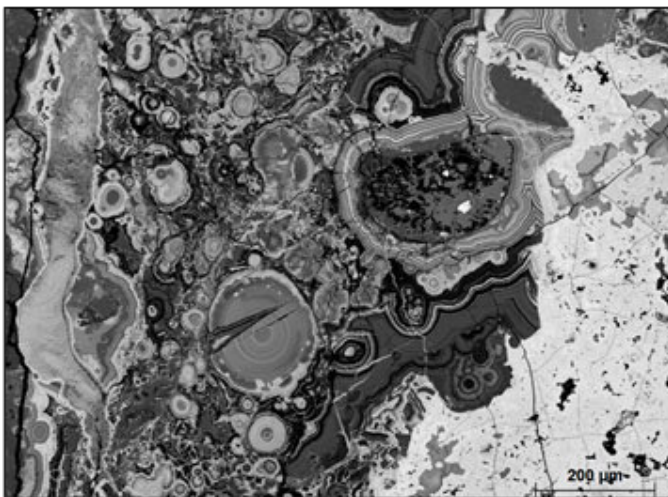


Figure 4. Colloidal cements at Taron.

Table 1. Minerals present in the Taron deposit. The major rock forming minerals are excluded from the table and the tabulated minerals are assemblages unique to the epithermal and alteration event. It is anticipated that additional and possibly new minerals will be discovered.

Cesian opal	$\text{SiO}_2 \cdot n\text{H}_2\text{O}$
Chalcedony	SiO_2
Goethite	$\alpha\text{-Fe}^{3+}\text{O}_9(\text{OH})$
Hematite	Fe_2O_3
Hollandite	$\text{Ba}(\text{Mn}^{4+}_6\text{Mn}^{3+}_2)\text{O}_{16}$
Coronadite	$\text{Pb}(\text{Mn}^{4+}_6\text{Mn}^{3+}_2)\text{O}_{16}$
Cryptomelane	$\text{K}(\text{Mn}^{4+}_7\text{Mn}^{2+})\text{O}_{16}$
Hollandite (supergroup)	$(\text{Ti}, \text{K}, \text{Ba}, \text{Zn}, \text{Cu})(\text{Mn}^{4+}, \text{Mn}^{3+})_8\text{O}_{16}$
Ramsdellite	MnO_2
Rancieite	$\text{Mg}_{0.29}\text{Mn}_{0.58}\text{O}_4 \cdot 1.7\text{H}_2\text{O}$
Todorokite	$(\text{Na}, \text{Ca}, \text{K}, \text{Ba}, \text{Sr})_{1-x}(\text{Mn}, \text{Mg}, \text{Al})_6\text{O}_{12} \cdot 3\text{-}4\text{H}_2\text{O}$
Romanechite	$(\text{Ba}, \text{H}_2\text{O})_2(\text{Mn}^{4+}\text{Mn}^{3+})_5\text{O}^{10}$
Pharmacosiderite	$(\text{Cs}, \text{Rb}, \text{K})\text{Fe}_4(\text{AsO}_4)_3(\text{OH})_4 \cdot 6\text{-}7\text{H}_2\text{O}$
Saialufite	$(\text{Na}, \text{Ca}, \text{Cu})_2\text{Mn}^{3+}_3\text{O}_2(\text{AsO}_4)_2(\text{CO}_3) \cdot 3\text{H}_2\text{O}$
Ludlockite	$\text{PbFe}_4\text{As}_{10}\text{O}_{22}$
Yukonite	$\text{Ca}_3\text{Fe}(\text{AsO}_4)_2(\text{OH})_3 \cdot 5\text{H}_2\text{O}$
Wallkilldellite	$\text{Ca}_4\text{Mn}^{2+}_3(\text{AsO}_4)_2(\text{OH})_4 \cdot 18\text{H}_2\text{O}$
Covellite	CuS

Cesium is predominantly hosted in pharmacosiderite; an arsenate mineral which can contain up to 12% Cs. Analysis with XRD and SEM indicate thallium is hosted within the manganate hollandite which can contain up to 3.4% Tl. Fp-XRF and point sample litho-geochemistry of individual mineral samples extracted from drill core show a positive correlation of Tl with Mn, K, Ba, Cu, and Zn – suggesting these elements are all present in hollandite's extensive solid solution.

The Taron Cesium-Thallium Epithermal Geyserite Deposit... *continued from page 15*

Geochemistry

In 2017, Cascadero Copper drilled 36 core holes in the Taron deposit. A geochemical database of 1239 samples was compiled from split two metre diamond drill hole interval assays that were analyzed at Bureau Veritas Labs in Vancouver. Their MA250 analytical procedure was used which combined 4-acid digestion with ICP-ES/ICP-MS analysis.

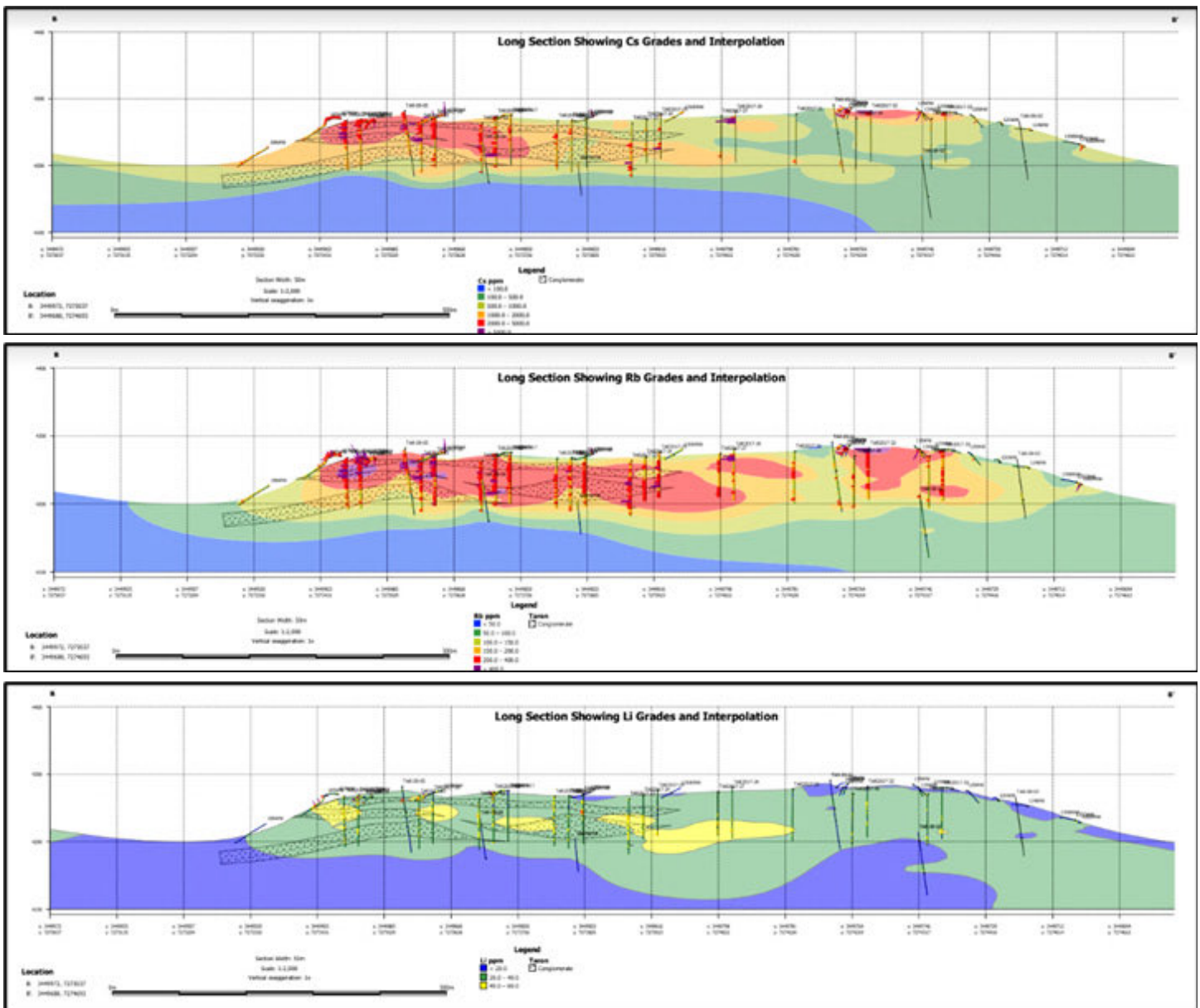
Because no specific standards were available to monitor the Cs analysis, Dr. B. Smee and CDN Resource Laboratories (CDN RL) were retained for the purpose of creating one. Pollucite from the Tanco Mine in Manitoba was utilized. Sample blanks were also provided by CDN RL.

Notable analytical values for bedrock samples from the Taron deposit are presented in Table 2 which shows high values for Cs, Rb, Li, Tl, As and Mn.

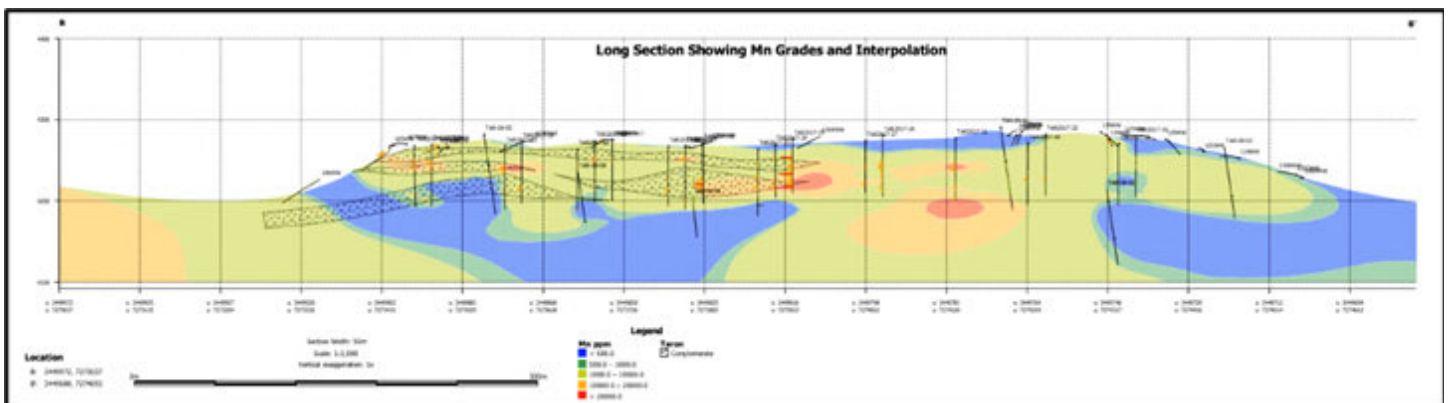
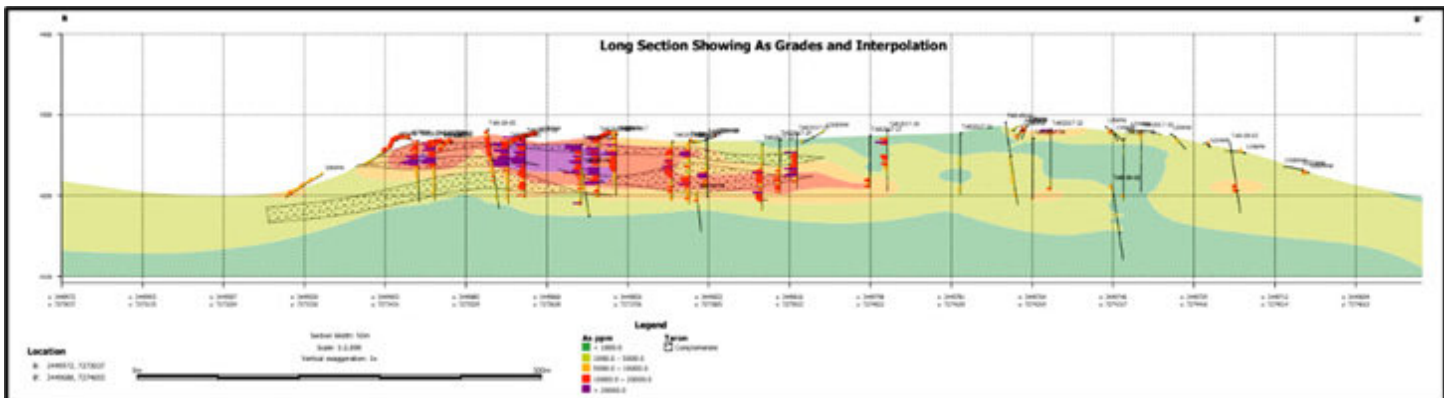
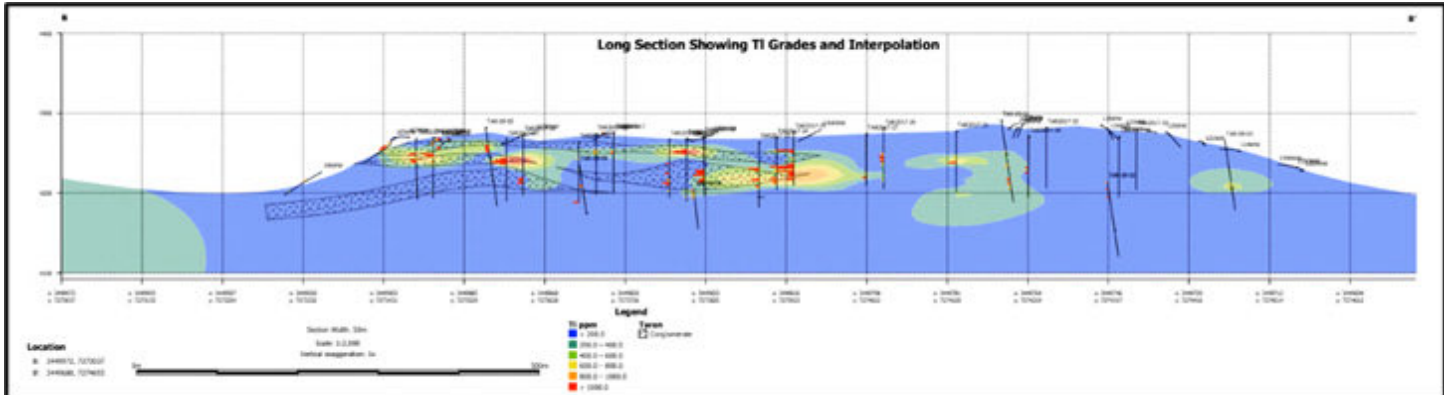
Table 2. Summary of analytical results for bedrock samples from the Taron deposit.

ppm	Minimum	Maximum	Mean	Median
Cs	52	15763	1406	1011
Rb	63	1364	221	194
Li	10	182	37	35
Tl	0.01	7440	229	31
As	5	57606	7482	4520
Mn	129	150089	6092	1050

Figure 5. Stacked sequence showing (top to bottom) concentrations of Cs, Rb, Li, Tl, As, and Mn across the deposit.



The Taron Cesium-Thallium Epithermal Geysierite Deposit... *continued from page 16*



Longitudinal sections, cross sections, and maps were plotted for the elements shown in Table 2. The simple geology, in the uppermost section of Figure 5, shows no control on the concentrations of the described elements and the mineralized envelope is essentially formless. It was hoped that the element distribution patterns would reveal the plumbing of the epithermal system around drill hole 2017-1 which was collared in travertine. A next logical choice is that the fault flanking the eastern side of mineralization provided a conduit for geysering and hot spring activity.

Discussion and Conclusions

Normally, fractionating granitic systems of an S-type granite of a compositional equivalent to the Macusani glass (Barnes *et al.* 1970) would be expected to crystallize minerals accommodating Li, Rb, and Cs (Large Ion Lithophile Elements) in that sequence as magmas pass through the solidus and subsolidus, hydrothermal stages. At Taron, a reversal of process is seen such that extremely high fractionated elements such as TI, Mn, and Cs are present in high concentrations.

To explain this observation, the authors took appropriate and comparable element data from Taron (Table 3) and normalized it to averaged Macusani glass (Barnes *et al.* 1970; Pichivant *et al.* 1987). The resulting spider plot is shown in Figure 6. Of interest is the Li, Rb, and Cs plot which suggests a reversely fractionating system.

The Taron Cesium-Thallium Epithermal Geysirite Deposit... *continued from page 17*

Figure 6. Spider plot of the Taron bedrock data normalized to the Macusani glass.

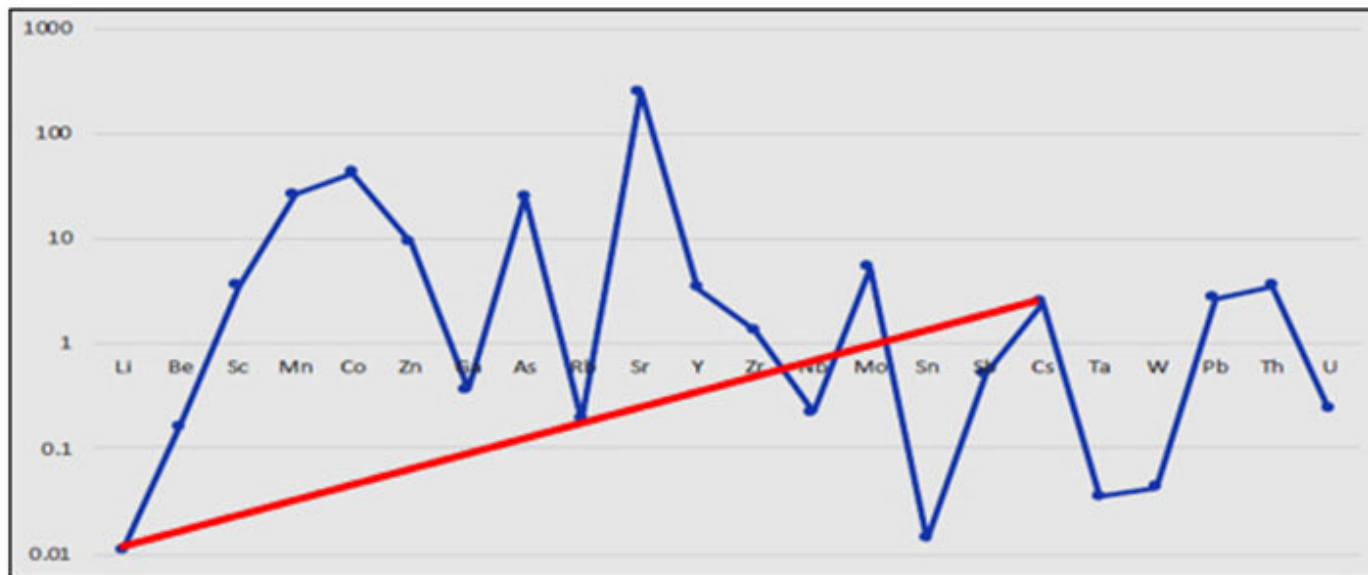


Table 3. Mean values for selected elements at Taron and the Macusani glass. Data for the Macusani glass are the high values from the given ranges of Barnes *et al.* (1973) assuming that the higher values represent a better dissolution method. Oxide data from Barnes *et al.* (1973) were converted back to elemental values.

ppm	Taron	Macusani glass
Li	37	3404
Be	6.6	41.1
Sc	8	2.2
Mn	6092	465
Co	29.9	0.71
Zn	861	97
Ga	15.5	42.4
As	7842	314
Rb	221	1179
Sr	359	1.62
Y	16.8	5.16
Zr	48	39
Nb	9.9	44
Mo	2.6	0.4
Sn	2.5	194
Cs	1406	566
Ta	0.9	26.9
W	3.1	73
Pb	22.6	7
Th	9.8	2.3
U	6.5	23.1

Two processes appear to have been operative at Taron: (1) remelting of an S-type granite or partial anatexis, reversing an expected fraction in the freezing of the same, and epithermal circulation of pregnant fluids to a place of geysering or hot spring circulation where the epithermal minerals formed and (2) selective concentration of Cs in pharmacosiderite.

At Yellowstone National Park, USA, Li- and Rb-bearing lepidolite and Cs-bearing analcime greisens are actively forming in sedimentary and volcanic rocks (Bargar & Beeson 1981, 1985) and considered by Keith *et al.* (1983) to be formed from hydrothermal fluid circulation through the voluminous underlying rhyolites and volcanic detritus.

Much has been written on the subject of microbial uptake of Cs (Zhao *et al.* 2005; Kong *et al.* 2007) for example, at Targejia, Tibet. At Taron, the authors explain the morphology of pharmacosiderite, a normally isometric mineral, by appealing to microbial action, leaving what are interpreted to be fossil casts (Fig. 7) containing as much as 12% Cs.

Thallium concentrations of up to 3.4% rocks are unknown in the literature and research is being conducted at the University of British Columbia to determine its mineral hosts. Future research should also consider the mineral form of fluorine and boron. Metallurgical samples from Taron assayed 540 to 1727 ppm F and the boron mineral, ulexite, was seen forming in warm springs in the local area. The Taron deposit warrants more research into its origin, mineralogy, geochemistry and metallurgy with the goal of resource development.

The Taron Cesium-Thallium Epithermal Geysirite Deposit... *continued from page 18*

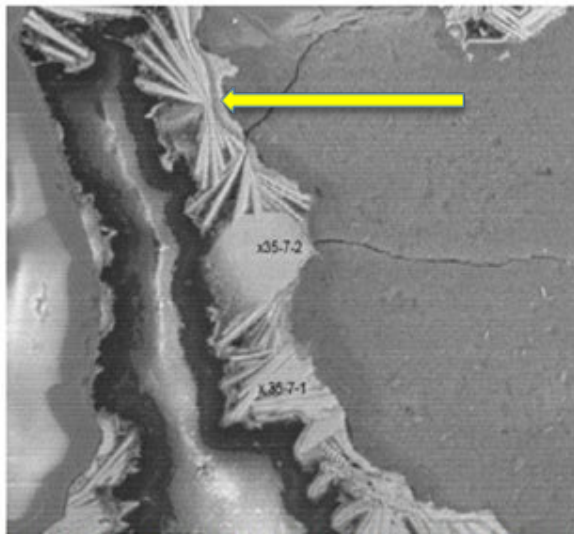


Figure 7. Arrow indicates microbe fossil casts(?) consisting of 10.6% to 11.5% Cs in pharmacosiderite casts. SEM back scattered image field of view is 0.4 mm.

It is also interesting to note at Spor Mountain, Utah, for example, in cycles of S-type rhyolitic volcanism, that the first cycle contains more enriched large ion lithophile elements and high field strength elements but are relatively depleted in the second cycle (Lindsey 1975; Burt *et al.* 1981).

Acknowledgements

Cascadero Copper Corporation is acknowledged and thanked for permission to write this paper. Barry Smee and the late Peter Winterburn are recognized for their support. Charles Parkinson kindly modelled the Taron trench and drill core data for the authors.

References

- Barnes, V.E., Edwards G., McLaughlin, W.A., Friedman, I., & Joensuu, O. 1973. Macusanite occurrence, age, and composition, Macusani, Peru. *Bulletin Geological Society America*, **81**, 1539-1546.
- Bargar, K.E. & Beeson, M.H. 1981. Hydrothermal alteration in research drill hole Y-2, Lower Geyser Basin, Yellowstone National Park, Wyoming. *American Mineralogist*, **66**, 473-490.
- Bargar, K.E. & Beeson, M.H. 1985. Hydrothermal Alteration in Research Drill hole Y-3, Lower Geyser Basin, Yellowstone National Park, Wyoming. *United States Geological Survey Professional Paper* **1054-C**.
- Burt, D.M. & Sheridan, M.F. 1981. Model for the formation of uranium/lithophile element deposits in fluorine-rich volcanic rocks. *In: Goodell, P. and Waters, A.C. (eds) Uranium in volcanic and volcanoclastic rocks*. American Association of Petroleum Geology **13**, 99-109.
- Chowdry, A.N., Handa, B.K. & Das, A.K. 1974. High lithium, rubidium, and cesium contents of thermal water, spring sediments, and borax deposits in the Puga Valley, Kashmir, India. *Geochemical Journal*, **8**, 61-65.
- Dahlquist, G. 2017. Foundations for a geochemical characterization of mudpots in Yellowstone National Park. Montana Technical Library.
- Hamilton, C. 2005. A mineralogical investigation of a cesium-bearing ore sample (105/WW) from the Taron Property. Internal report prepared for Argentine Frontier Resources Inc. by SGS Mineral Services, Dec. 16, 2005.
- Keith, T.E.C., Thompson, J.M. & Mays, R.E. 1983. Selective concentration of cesium during hydrothermal alteration, Yellowstone National Park, Wyoming. *Geochimica and Cosmochimica Acta*, **47**, 795-804.
- Kong F, Wang H, Zheng M., & Zheng, X. 2007. Isolation and characterization of thermophiles from Hot Springs at Dagejia cesium-bearing geysirite in Tibet. *Acta Geologica Sinica*, **81**, 1750-1753.
- Le Couteur, P. 2009. Petrographic report on a thallium-bearing Sample from the Taron Property, Argentina, Internal Report prepared for Argentine Frontier Resources Inc., Nov. 21, 2009.
- Ledoux, T.J., Winterburn, P.A., Downing, B.W., Trueman, D. & Hart, C.J.R. 2020. Department of thallium and cesium in the Taron epithermal cesium deposit: A new type of alkali-metal enriched deposit. AME Roundup 2020, January 20th, 2020, Vancouver, Poster #69.
- Lindsey, D.A. 1981. Volcanism and uranium mineralization at Spor Mountain, Utah. *In: Goodell, P. & Waters, A.C. (eds), Uranium in volcanic and volcanoclastic rocks*. American Association of Petroleum Geology, **13**, 89-98
- Pichivant, M., Herrera, J.V., Boulmier, S., Briqueu, L., Joron, J-L., Martine, J., Marin, L., Michard, A., Sheppard, S.M.F, Treuil, M. & Vernet, M. 1987. The Macusani glasses, SE Peru: evidence of chemical fractionation in peraluminous magmas. *In: Mysen, B.O. (ed) Magmatic Processes: Physicochemical Principles*, Geochemical Society, Special Publication No. 1.
- Richards, T. 2005. Taron alkali metal deposit. Internal report for Argentine Frontier Resources Inc. and Salta Exploraciones SA.
- Simpson, R. 2017. Technical Report NI 43-101 Salta Province, Argentina, unpublished report for Cascadero Copper, available on System for Electronic Disclosure and Reporting (SEDAR). https://www.sedar.com/homepage_en.htm
- Zhao, Y., Han, J., Guo, L., Qian, Z., Zhou, Y., Nie, F., & Li, Z. 2008. Characteristics and geological significance of mineralogy and fabrics for the hot spring cesium deposit occurring within the Targejia district, Tibet. *Acta Petrologica Sinica*, **24**, 519-530.